

# Threshold-Based Vehicle Detection Method for Distributed ISAC-Enabled V2X Networks

1<sup>st</sup> Han-Gyeol Lee, 2<sup>nd</sup> Kanghaeng Lee, 3<sup>rd</sup> Jingon Joung

*School of Electrical and Electronics Engineering*

*Chung-Ang University*

Seoul 06974, South Korea

{forener; qwezxc223211; jgjoung}@cau.ac.kr

**Abstract**—In this paper, a threshold-based vehicle detection method is proposed for decentralized integrated sensing and communication-enabled vehicle-to-everything networks. In the proposed detection method, a roadside unit (RSU) detects the vehicle by comparing a predetermined threshold with the energy of echo signals generated during communication between the neighboring RSU and the vehicle, i.e., passive sensing. To determine the detection threshold for reliable vehicle detection, closed-form expressions for detection and false-alarm rates are derived. The numerical results validate the accuracy of the analytical expressions derived and demonstrate that reliable vehicle detection can be achieved by selecting an appropriate detection threshold.

**Index Terms**—Integrated sensing and communication (ISAC), massive multiple-input multiple-output (mMIMO), millimeter-wave (mmWave), passive detection, vehicle-to-everything (V2X).

## I. INTRODUCTION

VEHICLE-TO-EVERYTHING (V2X) is a technology that enables vehicles to exchange information with adjacent vehicles, devices, and roadside units (RSUs) through wireless communications [1], [2]. Millimeter-wave (mmWave) and massive multiple-input multiple-output (mMIMO) technologies have been widely applied to V2X networks to enhance performance. With these technologies, the V2X network can adopt a highly directional beamforming, which reduces interference and improves spectral efficiency [3].

Recently, integrated sensing and communication (ISAC)-enabled mmWave mMIMO V2X networks have been thoroughly studied as next-generation V2X networks [3]. The ISAC is a framework that uses a unified radio waveform and hardware to perform communication and sensing simultaneously [2], [4], [5], [6]. In mmWave mMIMO V2X networks, the wide bandwidth and large antenna array facilitate accurate estimation of sensing information, such as distance, velocity, angle, and vehicle presence. Therefore, RSUs and vehicles in the mmWave mMIMO V2X network can accurately estimate the sensing information when the ISAC framework is incorporated into the network. Using sensing information, mmWave mMIMO V2X networks can significantly improve beamforming performance [7].

This work was supported in part by the National Research Foundation of Korea(NRF) grant funded by the Ministry of Science and ICT (RS-2024-00405510) and in part by Basic Research Program through the NRF of Korea funded by the Ministry of Education (RS-2025-25397301).

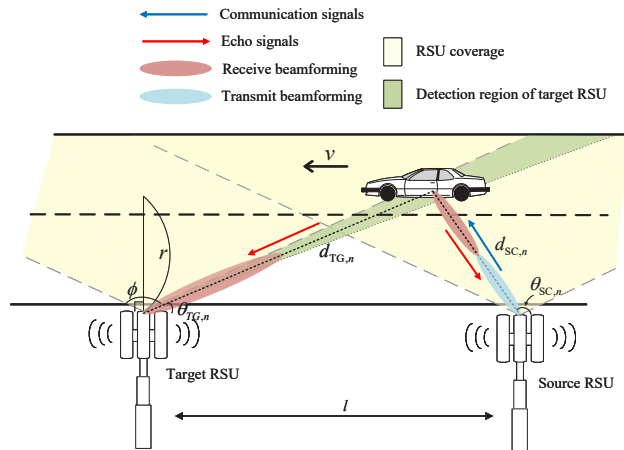


Fig. 1: Geometrical configuration of considered V2X network.

In mmWave mMIMO ISAC-enabled V2X networks, a backhaul for inter-RSU signaling and cooperation are generally assumed [3]; however, backhaul deployment could be unavailable due to high costs and complexity in practical V2X networks [8]. Furthermore, centralized operation through coordination increases network latency. Nevertheless, decentralized ISAC-enabled V2X networks, in which each RSU independently operates based on locally observed information [9], remain largely unexplored.

To fill the research gap, this paper proposes a passive vehicle detection method for decentralized ISAC-enabled mmWave mMIMO V2X networks. In the proposed detection method, the RSU detects the vehicle by performing energy detection on the echo signals generated during communication between the neighboring RSU and the vehicle. To achieve reliable detection, this paper derives closed-form expressions for the detection and false-alarm rates in vehicle detection. The numerical results validate the accuracy of the derived analytical expressions and demonstrate that reliable vehicle detection is feasible by selecting an appropriate detection threshold.

## II. SIGNAL AND SYSTEM MODELS

Fig. 1 illustrates a decentralized ISAC-enabled mmWave mMIMO V2X network. For simplicity, a scenario with two RSUs, specifically a source RSU and a target RSU, is consid-

ered where these RSUs are separated by  $l$  without backhaul connectivity. Due to the absence of backhaul links, the RSUs operate independently without information exchange. Each RSU covers an angular sector of width  $\phi$ , and the coverage areas of two RSUs partially overlap to maintain a seamless communication link. Each RSU is equipped with  $N_{\text{tx}}$  transmit and  $N_{\text{rx}}$  receive uniform linear array (ULA) antennas. A single vehicle travels at constant speed  $v$  along a straight road with a lateral distance  $r$ . Wireless communication between the source RSU and the vehicle is established through the line-of-sight channel. The communication process comprises  $N$  discrete time slots, each with a duration of  $\Delta T$ . To overcome severe pathloss and beam misalignment in mmWave V2X networks, the source RSU and vehicle adopt the predictive beamforming framework proposed in [7], which ensures reliable communication. In this setup, the target RSU passively detects the vehicle using echo signals without affecting communication link. Therefore, this paper focuses on the vehicle detection performance at the target RSU.

At the  $n$ th time slot, the source RSU transmits the downlink communication signals given by [7]

$$\mathbf{s}_n(t) = \sqrt{N_{\text{tx}}P_n}\mathbf{a}(N_{\text{tx}}, \hat{\theta}_{SC,n})x_n(t) \in \mathbb{C}^{N_{\text{tx}} \times 1}, \quad (1)$$

where  $P_n \in \mathbb{R}$  is the transmit power of the source RSU;  $x_n(t) \in \mathbb{C}$  represents the data signals;  $\hat{\theta}_{SC,n}$  is the prediction of the incident angle from the source RSU to the vehicle denoted by  $\theta_{SC,n} \in [-\frac{\pi}{2}, \frac{\pi}{2}]$ ; and  $\mathbf{a}(N, \theta)$  denotes the steering vector with the direction of angle  $\theta$ , written as

$$\mathbf{a}(N, \theta) = \frac{1}{\sqrt{N}} [1 \ e^{-j\pi \cos(\theta)} \ \dots \ e^{-j\pi(N_{\text{tx}}-1)\cos(\theta)}]^T \in \mathbb{C}^{N \times 1}. \quad (2)$$

Here, the antenna spacing of the ULA is set to half a wavelength of the carrier frequency. While the vehicle moves within the coverage of the source RSU, the target RSU observes the echo signals reflected from the vehicle, expressed as

$$\mathbf{r}_n(t) = \sqrt{N_{\text{tx}}P_n}\beta_n e^{j2\pi\mu_n t}\mathbf{a}(N_{\text{tx}}, \theta_{TG,n})\mathbf{a}^H(N_{\text{tx}}, \theta_{SC,n}) \times \mathbf{s}_n(t - \tau_n) + \mathbf{z}_n(t) \in \mathbb{C}^{N_{\text{rx}} \times 1}, \quad (3)$$

where  $\theta_{TG,n} \in \mathbb{R}$  is the incident angle from the target RSU to the vehicle;  $\mathbf{z}_n(t)$  is the additive white Gaussian noise (AWGN) vector following  $\mathcal{CN}(0, \sigma_z^2 \mathbf{I}_{N_{\text{rx}}})$  with the noise variance  $\sigma_z^2$ ;  $\tau_n \in \mathbb{R}$  is the propagation delay;  $\mu_n \in \mathbb{R}$  is the Doppler shift given by  $2v \cos(\theta_{TG,n})f_c/c$  for the carrier frequency  $f_c$  and the speed of light  $c$ ; and  $\beta_n \in \mathbb{C}$  represents the complex reflection coefficient given by  $\frac{\epsilon}{d_{TG,n} + d_{SC,n}}$ . Here,  $d_{SC,n}$  and  $d_{TG,n}$  are the distances from the vehicle to the source RSU and the target RSU, respectively, and  $\epsilon \in \mathbb{C}$  is the complex radar cross section.

### III. VEHICLE DETECTION IN TARGET RSU

#### A. Received Echo Signals with Monitoring Beamforming

The target RSU detects the vehicle without signaling from the source RSU. For this purpose, the target RSU performs receive beamforming steered to the entry angle of its coverage, which is hereafter referred to as monitoring beamforming. The monitoring beamforming concept enables the target RSU to

detect the vehicle while it moves within the detection region. The detection region is defined as the angular region where the echo signals from the vehicle can be observed, as illustrated by the green-shaded region in Fig. 1. Specifically, the monitoring beamformer is steered to an angle  $\psi = 0.5(\pi - \phi)$ . The target RSU applies matched filtering to the received echo signals to estimate propagation delay and Doppler shift, followed by energy detection to confirm the vehicle's presence. During this procedure, the combined echo signals are given by

$$\begin{aligned} \mathbf{r}_n(t) &= \sqrt{N_{\text{rx}}}\mathbf{a}^H(N_{\text{rx}}, \psi)\mathbf{r}_n(t) \\ &= \sqrt{K_n}\zeta_{TG,n}\xi_{SC,n}x_n(t - \tau_n)e^{j2\pi\mu_n t} + \mathbf{z}_n(t) \in \mathbb{C}, \end{aligned} \quad (4)$$

where  $K_n = N_{\text{rx}}N_{\text{tx}}P_n\beta_n^2$  is the effective array gain;  $\mathbf{z}_n(t) = \sqrt{N_{\text{rx}}}\mathbf{a}^H(N_{\text{rx}}, \psi)\mathbf{z}_n(t)$  is the combined AWGN distributed as  $\mathcal{CN}(0, \sigma_z^2)$ ;  $\zeta_{TG,n} = \mathbf{a}^H(N_{\text{rx}}, \psi)\mathbf{a}(N_{\text{rx}}, \theta_{TG,n})$  represents the receive beamforming gain of the target RSU; and  $\xi_{SC,n} = \mathbf{a}^H(N_{\text{tx}}, \theta_{SC,n})\mathbf{a}(N_{\text{tx}}, \hat{\theta}_{SC,n})$  denotes the transmit beamforming gain of the source RSU.

To estimate propagation delay and Doppler shift, the target RSU can adopt the matched filtering approach with a shifted version of transmitted signals [7]. However, noting that the source and target RSUs operate independently without any information exchange, full information of  $\mathbf{s}_n(t)$  is unavailable at the target RSU. In this paper, it is assumed that the target and source RSU share common reference signals contained in  $x_n(t)$ , denoted by  $c(t)$ . Using these common reference signals, the target RSU performs the matched filtering as follows:

$$\begin{aligned} \tilde{\mathbf{r}}_n(\tau, \mu) &= \int_0^{\Delta T} \mathbf{r}_n(t)c^*(t - \tau)e^{-j2\pi\mu_n t} dt \\ &= \sqrt{K_n}\zeta_{TG,n}\xi_{SC,n}\tilde{x}_n(\tau, \mu) + \tilde{\mathbf{z}}_n(\tau, \mu) \in \mathbb{C}, \end{aligned} \quad (5)$$

where  $\tilde{x}_n(\tau, \mu)$  and  $\tilde{\mathbf{z}}_n(\tau, \mu)$  correspond to the signal and noise components in the matched filtering output, respectively, written as

$$\tilde{x}_n(\tau, \mu) = \int_0^{\Delta T} x_n(t - \tau_n)c^*(t - \tau)e^{-j2\pi(\mu - \mu_n)t} dt \in \mathbb{C}, \quad (6)$$

$$\tilde{\mathbf{z}}_n(\tau, \mu) = \int_0^{\Delta T} \mathbf{z}_n(t)c^*(t - \tau)e^{-j2\pi\mu t} dt \in \mathbb{C}. \quad (7)$$

Here,  $\tilde{\mathbf{z}}_n(\tau, \mu)$  can be modeled by a zero-mean complex Gaussian random variable following  $\mathcal{CN}(0, a\sigma_z^2)$ , where  $a \in \mathbb{R}$  is a scaling factor to include the effect of matched filtering on noise [7]. Typically, reference signals have a pseudorandom structure with impulse-like correlation properties [10]. In this case, matched filtering amplifies the noise by the matched-filtering gain [11]. Therefore, the scaling factor can be represented as  $a = \rho G$  where  $\rho$  denotes the power ratio of  $c(t)$  to  $x_n(t)$  and  $G = \int_0^{\Delta T} |x_n(t)|^2 dt$  represents the matched filtering gain with respect to  $x_n(t)$ . Using  $\tilde{\mathbf{r}}_n(\tau, \mu)$  in (5), the target RSU estimates  $\tau_n$  and  $\mu_n$  as

$$(\hat{\tau}_n, \hat{\mu}_n) = \arg \max_{\tau \in \mathcal{T}, \mu \in \mathcal{M}} |\tilde{\mathbf{r}}_n(\tau, \mu)|^2, \quad (8)$$

where the search regions are given by  $\mathcal{T} = (0, \tau_{\max}]$  and  $\mathcal{M} = [-\mu_{\max}, \mu_{\max}]$  for the maximum propagation delay  $\tau_{\max}$  and

the maximum Doppler shift  $\mu_{\max}$ . In this paper,  $\tau_{\max}$  and  $\mu_{\max}$  are assumed to be known in the target RSU.

Based on propagation delay and Doppler shift estimates, the received echo signal power is obtained at the target RSU. Specifically, the target RSU measures the energy of the received echo signals as follows:

$$\begin{aligned}\tilde{R}_n &= |\tilde{x}_n(\hat{\tau}_n, \hat{\mu}_n)|^2 \\ &= |\sqrt{K_n} \zeta_{\text{TG},n} \xi_{\text{SC},n} \tilde{x}_n(\hat{\tau}_n, \hat{\mu}_n) + \tilde{z}_n(\hat{\tau}_n, \hat{\mu}_n)|^2,\end{aligned}\quad (9)$$

As confirmed in [7], predictive beamforming provides highly accurate angle prediction, leading to  $|\xi_{\text{SC},n}|^2 \approx 1$ . The monitoring beamforming gain  $\zeta_{\text{TG},n}$  is significant when the vehicle approaches the entry angle of the overlapped region, since the monitoring beam is steered toward this direction. With accurate beamforming, the mmWave mMIMO V2X system attains a substantial array gain from the large antenna array. This gain enables reliable estimation of the propagation delay and Doppler shift, such that  $\hat{\tau}_n \approx \tau_n$  and  $\hat{\mu}_n \approx \mu_n$ , which yields a matched filtering gain close to the ideal case, i.e.,

$$|\tilde{x}(\hat{\tau}_n, \hat{\mu}_n)|^2 \approx |\tilde{x}(\tau_n, \mu_n)|^2 = \rho G. \quad (10)$$

Furthermore, the array gain sustains a high effective signal-to-noise ratio (SNR) in the estimation of  $\tau_n$  and  $\mu_n$ , i.e.,  $K_n |\zeta_{\text{TG},n}|^2 \gg \sigma_z^2$ . Therefore,  $\tilde{z}_n(\hat{\tau}_n, \hat{\mu}_n)$  in (9) is negligible and  $\tilde{R}_n$  can be approximated when the vehicle is near the entry angle of the overlapped region as follows:

$$\begin{aligned}\tilde{R}_n &\approx K_n G_n |\zeta_{\text{TG},n}|^2 \\ &\stackrel{(a)}{=} K_n G_n |\Lambda(N_{\text{rx}}, \cos(\theta_{\text{TG},n}) - \cos(\psi))|^2,\end{aligned}\quad (11)$$

where (a) is derived from that the mismatched beamforming gain, i.e.,  $\zeta_{\text{TG},n}$  in this case, is generally represented with respect to the Dirichlet sinc function  $\Lambda(N, x)$  given by  $\Lambda(N, x) = \frac{\sin(\frac{\pi}{2} Nx)}{N \sin(\frac{\pi}{2} x)}$  [12]. Fig. 2 illustrates  $\tilde{R}_n$  in (11) across the location of the vehicle. As the vehicle approaches the target RSU,  $\theta_{\text{TG},n}$  gradually aligns with  $\psi$ , accordingly, increasing  $\tilde{R}_n$ . Furthermore,  $\tilde{R}_n$  maintains non-negligible values while the vehicle moves within the detection region. This observation indicates that the target RSU can detect the vehicle before it reaches the overlapped region.

### B. Detection Performance Analysis

Vehicle detection can be achieved through the energy detection of the received echo signals. Herein, we omit  $\tau$ ,  $\mu$ ,  $\theta$ , and associated parameters to avoid clutter unless otherwise specified. When the vehicle is present in the detection area, the vehicle echo signal arrives at the target RSU, increasing the received echo signal energy in (11). If the vehicle is absent, the target RSU measures the energy of the received echo signal as  $|\tilde{z}_n|^2$ . Therefore, the vehicle detection problem is formulated as an energy detector in  $\tilde{R}_n$  [13]. In this problem, the detection threshold is determined by the detection rate and the false alarm rate. Specifically, the detection rate and the false alarm rate are defined as

$$P_D(\Gamma) \triangleq P(|\tilde{s}_n + \tilde{z}_n|^2 > \Gamma), \quad (12)$$

$$P_F(\Gamma) \triangleq P(|\tilde{z}_n|^2 > \Gamma), \quad (13)$$

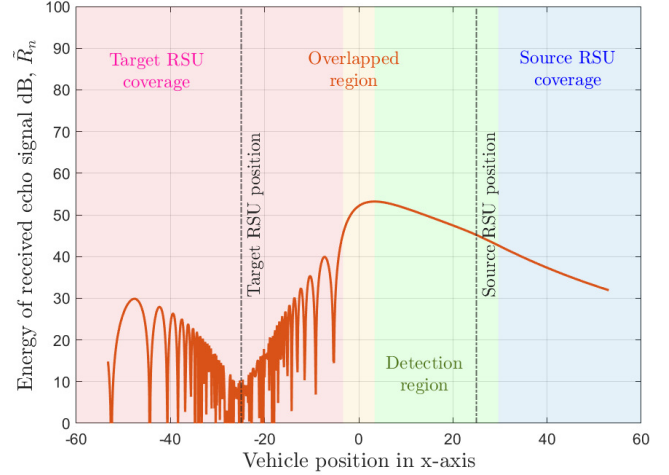


Fig. 2: Energy of received echo signal across vehicle position when  $N_{\text{tx}} = N_{\text{rx}} = 128$ ,  $r = 6$  m,  $\phi = 160^\circ$ ,  $\psi = 10^\circ$ ,  $l = 50$  m, and source and target RSU positions at 25 m and  $-25$  m, respectively, in x-coordinate.

where  $\tilde{s}_n = \sqrt{K_n} \zeta_{\text{TG},n} \xi_{\text{SC},n} \tilde{x}_n$  and  $\Gamma$  denotes the detection threshold. Invoking that  $\tilde{s}_n + \tilde{z}_n$  follows  $\mathcal{CN}(\tilde{s}_n, \rho G \sigma_z^2)$ ,  $|\tilde{s}_n + \tilde{z}_n|$  is distributed as a Rician distribution. Furthermore, from  $P_D(\Gamma) = P(|\tilde{s}_n + \tilde{z}_n| > \sqrt{\Gamma})$ , the detection rate can be represented by the complementary cumulative distribution function of the Rician distribution. Consequently,  $P_D(\Gamma)$  is obtained as [14]

$$P_D(\Gamma) = Q_1 \left( \sqrt{\frac{2\tilde{R}_n}{\rho G \sigma_z^2}}, \sqrt{\frac{2\Gamma}{\rho G \sigma_z^2}} \right), \quad (14)$$

where  $Q_1(x, y)$  is the first-order Marcum-Q function written as  $Q_1(x, y) = \int_y^\infty u \exp\left(-\frac{u^2 + x^2}{2}\right) I_0(ux) du$  for the zeroth-order modified Bessel function of the first kind  $I_0(\cdot)$ . Subsequently,  $P_F(\Gamma)$  is the special case of  $P_D(\Gamma)$  with  $\tilde{s}_n = 0$  or equivalently  $\tilde{R}_n = 0$ . Therefore, the false alarm rate is given by [15]

$$P_F(\Gamma) = Q_1 \left( 0, \sqrt{\frac{2\Gamma}{\rho G \sigma_z^2}} \right) = \exp\left(-\frac{\Gamma}{\rho G \sigma_z^2}\right). \quad (15)$$

By examining both (14) and (15), the detection threshold  $\Gamma_{\text{th}}$  is selected to achieve a low  $P_F(\Gamma_{\text{th}})$  while maintaining a sufficiently high  $P_D(\Gamma_{\text{th}})$  [13]. With the chosen  $\Gamma_{\text{th}}$ , the target RSU determines the presence of a vehicle if  $\tilde{R}_n > \Gamma_{\text{th}}$  at least one time during the vehicle's movement within the detection region.

## IV. SIMULATION RESULTS

To verify the availability of vehicle detection, detection and false alarm rates are evaluated across different threshold values. During the simulations, the source RSU transmits the signals to the vehicle using the predictive beamforming in [7], while the target RSU detects the vehicle with the echo signals. The simulation parameters are listed in Table I. Specifically,

TABLE I: Simulation Parameters

Parameters	Values
Distance from RSU to road $r$	5 m
Distance between RSUs $l$	50 m
Position of source RSU in x-coordinate	25 m
Position of target RSU in x-coordinate	-25 m
RSU coverage angle $\phi$	160°
Vehicle speed $v$	160 km/h
Initial incident angle at target RSU $\theta_{TG,0}$	4.0843°
Initial distance at target RSU $d_{TG,0}$	84.2416 m
Initial reflection coefficient $\beta_0$	$\frac{\sqrt{2}}{2} + \frac{\sqrt{2}}{2}j$
Time slot duration $\Delta T$	1 ms
Carrier frequency $f_c$	30 GHz
System SNR $P_n/\sigma_z^2$	10 dB
Matched filtering gain of transmit signals $G$	10
Ratio of reference signals $\rho$	0.1

the perpendicular distance from the road to each RSU is  $r = 5$  m. The separation between the two RSUs is  $l = 50$  m. The x-coordinates of the source and target RSUs are set to 25 m and -25 m, respectively, with the origin at the midpoint. The angle of coverage of each RSU is set to  $\phi = 160^\circ$ . The speed of the vehicle is fixed by  $v = 160$  km/h. The initial vehicle location is set to have an incident angle of 10° relative to the source RSU. Accordingly, the initial geometry of the vehicle relative to the target RSU is given by the incident angle  $\theta_{TG,0} = 4.0843^\circ$  and the distance  $d_{TG,0} = 84.2416$  m. Other parameters include:  $\beta_0 = \frac{\sqrt{2}}{2} + \frac{\sqrt{2}}{2}j$ ,  $\Delta T = 1$  ms,  $f_c = 30$  GHz, SNR  $P_n/\sigma_z^2 = 10$  dB,  $G = 10$ , and  $\rho = 0.1$ .

Fig. 3 presents  $P_F(\Gamma)$  and  $P_D(\Gamma)$  in  $\Gamma$  for  $N_{tx} = N_{rx} = 16$  and 32. The shaded region labeled by threshold region indicates the range of  $\Gamma$  that simultaneously achieves a negligible  $P_F(\Gamma)$  while preserving a high  $P_D(\Gamma)$ . By selecting a value in this region as  $\Gamma_{th}$ , the reliable detection of vehicles at the target RSU can be achieved through the thresholding method. If no such threshold region exists,  $\Gamma_{th}$  is chosen according to alternative criteria, e.g., constant false alarm rate or generalized likelihood ratio test [13]. Furthermore, the close agreement between the Monte Carlo simulation and the theoretical expressions validates the accuracy of the formulas derived in (14) and (15). Consequently, a precise threshold selection can be achieved for reliable vehicle detection from (14) and (15).

## V. CONCLUSION

This paper proposed a passive vehicle detection method for decentralized ISAC-enabled mmWave mMIMO V2X networks. In the proposed detection method, the target RSU detects the vehicle without signaling from the source RSU, using the monitoring beamforming at the entry angle of its coverage. For threshold selection, closed-form expressions for detection and false-alarm rates are derived. The numerical results validated that reliable vehicle detection can be achieved by selecting an appropriate detection threshold based on the derived expressions of the detection and false-alarm rates.

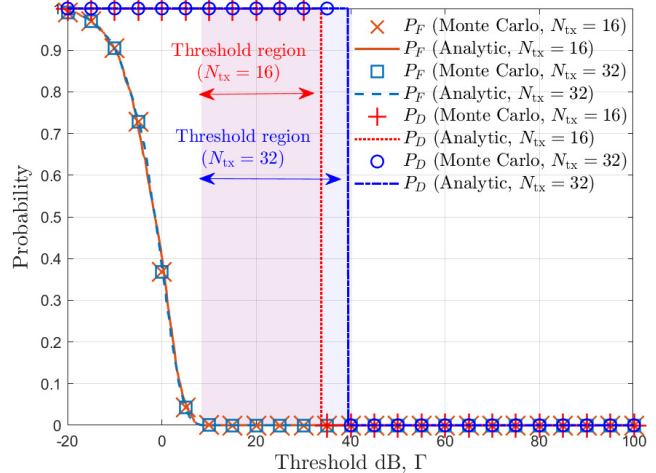


Fig. 3: Detection and false alarm rates across threshold value when  $N_{tx} = N_{rx} = 16$  and 32.

## REFERENCES

- [1] H. Yu and J. Joung, "Frame structure design for vehicular-to-roadside unit communications using space-time line code under time-varying channels," *IEEE Syst. J.*, vol. 15, no. 2, pp. 3150–3153, 2021.
- [2] J. Joung, H. Yu, and T. Q. Quek, "Integrated single target sensing and multiuser communications based on zero-forcing beamforming," *Veh. Commun.*, vol. 43, Oct. 2023, Art. no. 100637.
- [3] Z. Du, F. Liu, Y. Li, W. Yuan, Y. Cui, and Z. Zhang, "Toward ISAC-empowered vehicular networks: Framework, advances, and opportunities," *IEEE Wireless Commun.*, vol. 32, no. 2, pp. 222–229, Apr. 2025.
- [4] K. Kim, J. Kim, and J. Joung, "A survey on system configurations of integrated sensing and communication (ISAC) systems," in *Proc. Int. Conf. Inf. Commun. Technol. Converg. (ICTC)*, Jeju, Korea, Oct. 2022, pp. 1176–1178.
- [5] H.-G. Lee, C. K. Ho, and J. Joung, "WiFi sensing: Data-aided approach," in *Proc. IEEE Wireless Commun. Netw. Conf. (WCNC)*, Milan, Italy, Mar. 2025, pp. 1–6.
- [6] J. Kim and J. Joung, "Movable antenna-assisted integrated single-target passive sensing and multiuser communication systems," in *IEEE VTS Asia Pacific Wireless Comm. Symposium (APWCS)*, Tokyo, Japan, Aug. 2025, pp. 1–3.
- [7] F. Liu, W. Yuan, C. Masouros, and J. Yuan, "Radar-assisted predictive beamforming for vehicular links: Communication served by sensing," *IEEE Trans. Wireless Commun.*, vol. 19, no. 11, pp. 7704–7719, Nov. 2020.
- [8] B. Tezergil and E. Onur, "Wireless backhaul in 5G and beyond: Issues, challenges and opportunities," *IEEE Commun. Surveys Tuts.*, vol. 24, no. 4, pp. 2579–2632, 4th Quart. 2022.
- [9] H. Zhou, W. Xu, J. Chen, and W. Wang, "Evolutionary V2X technologies toward the internet of vehicles: Challenges and opportunities," *Proc. IEEE*, vol. 108, no. 2, pp. 308–323, Feb. 2020.
- [10] J. M. Velazquez-Gutierrez and C. Vargas-Rosales, "Sequence sets in wireless communication systems: A survey," *IEEE Commun. Surveys Tuts.*, vol. 19, no. 2, p. 1225–1248, 2nd Quart. 2017.
- [11] M. Pursley, "Performance evaluation for phase-coded spread-spectrum multiple-access communication - Part I: System analysis," *IEEE Trans. Commun.*, vol. 25, no. 8, pp. 795–799, Aug. 1997.
- [12] L. Afeef, H. M. Furqan, and H. Arslan, "Robust tracking-based PHY-authentication in mmwave MIMO systems," *IEEE Trans. Inf. Forensics Security*, vol. 19, pp. 10375–10386, Oct. 2024.
- [13] S. M. Kay, *Fundamentals of Statistical Signal Processing: Detection Theory*. vol. 2. Englewood Cliffs, NJ, USA: Prentice-Hall, 1998.
- [14] M. Z. Bocus, C. P. Dettmann, and J. P. Coon, "An approximation of the first order Marcum Q-function with application to network connectivity analysis," *IEEE Commun. Lett.*, vol. 17, no. 13, pp. 499–502, Mar. 2013.
- [15] M. K. Simon and M.-S. Alouini, *Digital Communication Over Fading Channels*. Hoboken, NJ, USA: Wiley, 2005.